

EXPANDING QUASARS AND THE EXPANSION OF THE UNIVERSE

MARSHALL H. COHEN, PETER D. BARTHEL, TIMOTHY J. PEARSON, AND J. ANTON ZENSUS

Owens Valley Radio Observatory, California Institute of Technology

Received 1987 October 7; accepted 1987 November 24

ABSTRACT

Thirty-two compact radio sources have both a redshift z and an internal proper motion, μ , measured with VLBI. These two observables are anticorrelated. There is a rough upper limit to $\mu(z)$ which falls much faster than $(1+z)^{-1}$, the function which describes the limiting proper motion in a simple model in which quasars are all at the same distance, and their various values of z reflect their peculiar velocities. Thus redshift is a measure of distance, unless there is a strong anticorrelation between z and the linear velocity of the VLBI components. Friedmann cosmology describes the upper limit, and a relativistic beam model gives $\gamma \sim 9-18$ for the Lorentz factor of the moving components, for $H_0 = 100-50 \text{ km s}^{-1} \text{ Mpc}^{-1}$. In this model most of the sources are aimed close to the line of sight, and Doppler boosting is probably responsible for this selection effect.

Relativistic shells expanding into dipole fields do not match the data, unless the Hubble constant is allowed to assume extreme values. Chronometric cosmology does not appear to describe the upper limit to the observed proper motions.

Subject headings: cosmology — quasars

I. INTRODUCTION

VLBI studies at centimeter wavelengths have shown that compact radio sources often have variable structure. In many cases the brightness distribution takes the form of two or more "components" which are strung along a well-defined line, and the variation consists of a secular increase in the separation of the components. Such sources have internal proper motions, measured in milliarcseconds (mas) per year. These are the objects under discussion in this paper. They have two measurable quantities, the proper motion, μ , and the redshift, z . First we discuss the relation between these observables; then we consider several kinematic models which might explain them.

A few sources with rapid variations in structure do not have well-defined motions, because the continuing identification of any given component is impossible. This was once the case, for example, with BL Lac, but when the observing interval was shrunk the components became identifiable and a proper motion was measured (Mutel and Phillips 1987). In the early measurements the observing interval apparently exceeded the evolution time. A current example is 3C 111, which has looked different at every observing session (Preuss and Alef 1987). No proper motion can be assigned to 3C 111, and it and similar objects are excluded from this paper.

In using the proper motion data, it has been customary to calculate an apparent transverse velocity, which frequently exceeds the speed of light. The word "superluminal" was coined to describe this situation. There is sometimes a tendency to think that this condition is somehow perverse and requires a special explanation. We avoid this by ignoring the numerical value of the apparent transverse linear velocity and dealing mainly with the proper motion, an observable.

II. THE DATA

The data we use are shown in Table 1, which is an updated version of the table published by Zensus and Pearson (1987); see Porcas (1987) for a similar compilation. The sources are drawn from a variety of samples with differing selection criteria, which include flux density, spectral index, variability, and

compactness, but not redshift. The selection is biased towards large proper motions, because whenever one of these is found (or suspected) it is monitored intensively. However, we are not aware of any selection biases which would couple the measured values of proper motion and redshift.

In Table 1 the proper motion, μ , (col. [4]) is given for the components shown in column (3) and is usually defined with respect to the core. In most cases the core is readily identified as a particularly compact, flat-spectrum component at one end of the brightness distribution. A recent reference for each source is given in column (8).

The quality of these measurements differs substantially from source to source owing to various factors, e.g., number of observing epochs (col. [5]), wavelengths of observation (col. [6]), and degree of complexity of the source structure; and therefore it would be difficult to assign error bars to the μ values. However, we have examined the evidence for proper motion in each case and placed the points in one of two categories (col. [7]). The filled circles represent sources with well-established measurements, i.e., based on maps at three or more epochs where the components are well identified. The crosses represent sources with only limited observations (e.g., less than three epochs, or only one baseline), or which have an ill-defined, complex source structure. The crosses also include three objects (1040 + 123, 1901 + 319, 2230 + 114) which appear to have separating components, but at the first of three observing epochs the separation was below the resolution limit.

The source 2230 + 114 was observed at a long wavelength, 32 cm, and there is a possibility that its variations are not intrinsic but are due to interstellar scintillation. Bååth (1987) mentions this possibility, but remarks that the object is at relatively high galactic latitude (-32°) and that scintillation is therefore unlikely. Other comments on individual sources in Table 1 are given as footnotes.

Figures 1a and 1b show the (μ, z) data from Table 1. We give both linear and logarithmic graphs to facilitate seeing the trends. Upper limits are indicated by arrows. The various lines refer to models which are discussed later.

TABLE 1
SOURCES WITH MEASURED INTERNAL PROPER MOTION

Source (1)	z (2)	Component (3)	μ (mas yr ⁻¹) (4)	Epochs (5)	λ (cm) (6)	Quality (7)	References (8)
0153 + 744	2.338	...	<0.03 ^a	5	6/18	•	1
0212 + 735	2.367	...	0.09 ^b	3	6	×	1
0316 + 413 3C 84	0.0172	...	0.24	3	2.8	•	2
0333 + 321 NRAO 140	1.258	B	0.15	4	2.8/6	•	3
0430 + 052 3C 120	0.033	A	1.35	4	2.8/6	•	4
0430 + 052	...	B	2.53	7	2.8/6	•	4
0430 + 052	...	C	2.47	5	2.8/6	•	4
0430 + 052	...	D	2.66	6	2.8/6	•	4
0430 + 052	...	E	2.54	4	2.8/6	•	4
0710 + 439	0.517	B	<0.04 ^c	2	6	×	5
0710 + 439	...	C	<0.07 ^c	2	6	×	5
0711 + 356	1.62	...	-0.05 ^d	2	6	×	6
0723 + 679 3C 179	0.846	...	0.19	7	2.8	•	7
0735 + 178	0.424	NE	0.18	3	1.3	×	8
0850 + 581	1.322	...	0.12	3	6	•	9
0851 + 202 OJ 287	0.306	SW1-2	0.28 ^e	2	6	×	10
0906 + 430 3C 216	0.669	...	0.17	3	6	×	5
0923 + 392 4C 39.25	0.699	a-c	<0.006	>8	2.8/3.6	•	11
0923 + 392	...	b	0.16	5	2.8/3.6	•	11
1040 + 123 3C 245	1.029	...	0.11 ^f	4	2.8	•	12
1137 + 660 3C 263	0.652	...	0.06	3	2.8	•	13
1150 + 812	1.25	...	0.13	3	6	•	1
1226 + 023 3C 273	0.158	C3	0.79	10	2.8/6	•	14
1226 + 023	...	C4	0.99	6	2.8/6	•	14
1226 + 023	...	C5	1.20	3	2.8	•	15
1226 + 023	...	C7a	0.76	3	2.8	•	15
1228 + 127 M87	20 Mpc	...	1.1	3	18	×	16
1253 - 055 3C 279	0.538	?	0.5 ^g	6	3.8	×	17
1253 - 055	...	B2	0.11	11	1.3/2.8/6	•	18
1637 + 826 NGC 6251	0.023	...	<0.3	2	18	×	19
1641 + 399 3C 345	0.595	C2	0.48	13	2.8/6	•	20
1641 + 399	...	C3	0.30	13	2.8/6	•	20
1641 + 399	...	C4	0.07, 0.3	6, 4	1.3/2.8	••	20
1642 + 690	0.751	...	0.34	2	6	×	21
1721 + 343 4C 34.47	0.206	...	0.36	2	6	×	22
1901 + 319 3C 395	0.635	1-2	<0.06	3	6	•	23
1901 + 319	...	3	0.64 ^f	3	6	×	23
1928 + 738	0.302	A1-4	0.6	7	6/18	•	24
1934 - 638	0.183	...	<0.03 ^h	2	13	×	25
1951 + 498	0.466	...	~0.07	2	2.8	×	26
2021 + 614	0.2266	...	<0.04	4	3.8/5/13	•	6
2134 + 004	1.936	...	<0.01 ⁱ	5	2.8/6	×	27
2200 + 420 BL Lac	0.0695	1-4	~0.76 ^j	13	2.8	•	28
2230 + 114 CTA 102	1.037	...	~0.65 ^k	3	32	×	29
2251 + 158 3C 454.3	0.859	2	<0.05	7	2.8	•	30
2251 + 158	...	4	0.35 ^h	4	2.8	×	30

^a Upper limit on separation of 12 mas double.

^b No published sequence of maps available yet.

^c One- σ limit; motion relative to component A.

^d Plotted as +0.05 in Fig. 1.

^e Polarization data.

^f Well-separated double only at two epochs.

^g One-baseline results.

^h Twelve yr limit.

ⁱ Complex structure.

^j Average of four events; possibly deceleration.

^k Long λ ; well-separated components only at two epochs.

REFERENCES.—(1) Witzel 1987; (2) Romney *et al.* 1984; (3) Marscher and Broderick 1985; (4) Walker 1986; (5) Pearson, Readhead, and Barthel 1987; (6) Readhead, Pearson, and Unwin 1984; (7) Porcas 1987; (8) B  ath 1984; (9) Barthel *et al.* 1986; (10) Roberts and Wardle 1987; (11) Shaffer and Marscher 1987; (12) Hough and Readhead 1987; (13) Zensus, Hough, and Porcas 1987; (14) Unwin *et al.* 1985; (15) Cohen *et al.* 1987b; (16) Biretta and Reid 1988; (17) Cotton *et al.* 1979; (18) Unwin 1987; (19) Jones 1986; (20) Biretta, Moore, and Cohen 1986; (21) Pearson *et al.* 1986; (22) Barthel 1987; (23) Simon *et al.* 1987; (24) Eckart *et al.* 1985; (25) A. K. Tzioumis, private communication; (26) Zensus and Porcas 1987; (27) Pauliny-Toth *et al.* 1984; (28) Mutel and Phillips 1987; (29) B  ath 1987; (30) Pauliny-Toth *et al.* 1987.

III. DISCUSSION

a) Regression

The points in Figure 1 do not make a scatter diagram, but appear to fall below an upper bound which decreases with z . In this regard Figure 1 is similar to diagrams which show "largest angular size" as a function of z (Kapahi 1987). To test the apparent decrease with redshift, we divided the data into bins of width 0.05 in $\log(1+z)$ and examined the regression of the largest μ -values in every bin. We restricted the calculation to the filled circles. Disregarding the upper limits, the null hypothesis (zero regression) is rejected at the 95% confidence level (one-tailed Student's t test). Including the upper limit at $z = 2.23$ gives $\log \mu_{\max} = 0.18 - (3.20 \pm 0.77) \log(1+z)$ and the confidence level increases to 99.5%.

b) Models

The redshift and the proper motion are statistically correlated. In this section we consider models which have been proposed to explain the redshift, and ask if they can explain this correlation.

i) Redshift Measures Velocity

Various suggestions have been made to the effect that quasars are not at cosmological distances. We examine that possibility by assuming that they are moving at high speed, and that their redshift is the normal effect of special relativity in Euclidean space. We first assume that the objects are all at the same distance, r , and that they are intrinsically the same. They shoot out luminous blobs with the same Lorentz factor γ but the nozzles are oriented at random, and the quasars themselves move with a variety of speeds and directions.

In an Appendix we show that for every direction of quasar motion, $\mu(z)$ has an upper limit. This limit is a minimum for quasars moving directly away from us, and is given by equation (A2). In Figure 1 we have plotted this as a dotted line $\mu \propto (1+z)^{-1}$, normalized to fit the higher points of 3C 120. The line does not even approximately match the data. This strongly suggests that z must be a measure of distance. The bad fit could also be explained if there were a hidden mechanism which produced an anticorrelation between z and γ , or a correlation between z and θ , the angle to the line of sight. We reject these possibilities, since the redshifts are determined from emission lines which arise in well-understood ways far from the centers of activity in the quasars.

Terrell (1975) has suggested a local theory in which quasars are all shot out of the galactic center at the same time, and those with higher redshift are now farther away. From equation (A2) and using $r = \beta ct$, where t is the time since the explosion and βc is the quasar velocity, we have an upper bound to the internal proper motion

$$\mu_m = \left[\frac{(1+z)^2 + 1}{(1+z)^2 - 1} \right] \left(\frac{1}{1+z} \right) \frac{\beta_b' \gamma_b'}{t} \quad (1)$$

where $\beta_b' c$ is the blob velocity relative to the quasar, and $\gamma_b' = [1 - (\beta_b')^2]^{-1/2}$. This relation is shown as the dotted curve marked "Local" in Figure 1. It is normalized to the top point in 3C 345, which gives $\beta_b' = 0.01$ for $t = 6 \times 10^6$ yr (Terrell 1975). This curve falls rapidly with z and could reasonably be an upper limit to the data.

ii) Chronometric Cosmology

In the chronometric cosmology (Segal 1979), the proper motion of objects with apparent separation velocity $\beta_{\text{chron}} c$ is

$\mu = 31.6(\beta_{\text{chron}}/R)(1+z)z^{-1/2}$, where R is the scale factor in Mpc, and μ is measured in mas yr^{-1} . To scale this to 3C 120 we adopt $(R/\beta_{\text{chron}}) = 65$ Mpc which, with $R = 60$ Mpc (Segal 1979), gives $\beta_{\text{chron}} = 0.92$. As Segal pointed out, the chronometric cosmology gives smaller transverse velocities, for a given proper motion, than does relativistic cosmology. In the standard cosmology 3C 120 has $\beta_{\perp} = 3.9$, for a Hubble constant of $H_0 = 100 \text{ km s}^{-1} \text{ Mpc}^{-1}$.

The expression $\mu(z)$, with $(R/\beta_{\text{chron}}) = 65$ Mpc, is plotted in Figure 1 as a dotted line. It does not form a good upper envelope to the data points, and implies a strong evolution of velocity with z . Specifically, the NRAO 140 point ($z = 1.258$) corresponds to $\beta_{\text{chron}} = 0.14$, while the highest 3C 120 point ($z = 0.033$) corresponds to $\beta_{\text{chron}} = 0.89$. We conclude that the chronometric cosmology is unable to explain the data, unless the powerful evolution of velocity with z can be explained.

iii) Relativistic Cosmology; Jets

Assume that z measures distance in a Friedmann universe, and that we are dealing with thin randomly oriented jets containing luminous blobs all moving with the same γ . Then the observed proper motions will have an upper envelope given by (e.g., Pearson and Zensus 1987)

$$\mu = 2.11 \times 10^{-4} \beta \gamma H_0 g(q_0, z) \text{ mas yr}^{-1}, \quad (2)$$

where $g(q_0, z)$ is given by

$$g(q_0, z) = q_0^2(1+z)[q_0 z + (q_0 - 1)(\sqrt{1 + 2q_0 z} - 1)]^{-1}. \quad (3)$$

The solid line in Figure 1 represents equation (2) for $\gamma H_0 = 900 \text{ km s}^{-1} \text{ Mpc}^{-1}$ and $q_0 = 0.5$, assuming $\gamma^2 \gg 1$. This curve could reasonably well form an upper limit to the data. We expect that in reality there would be a distribution in γ , so a sharp boundary is not expected. The two high points (CTA 102 and 3C 395) need confirmation, but if taken at face value require $\gamma H_0 \sim 1800$.

The dashed line in Figure 1 shows $\mu(z)$ for the special case $H_0 = 100 \text{ km s}^{-1} \text{ Mpc}^{-1}$, $q_0 = 0.5$, $\gamma = 4$, $\theta = 60^\circ$. Any source which has $\gamma = 4$ but $\theta > 60^\circ$ lies below the line, and those with $\theta < 60^\circ$, except the ones within a small cone about the line of sight, lie above the line. Therefore, the "median line" for sources oriented at random would be slightly below the dashed line in Figure 1. The median lines for $\gamma \geq 4$ are all very close together, while for $\gamma < 4$ they drop below the dashed line. If $H_0 < 100$, or if $q_0 < 0.5$, the median lines also move down. Thus we would expect less than half the points to lie above the dashed line. This is obviously not the case, and we conclude that the sources in the figure must be predominantly aligned in our direction.

There evidently is some mechanism at play which biases our selection of objects toward those which are pointing at us. We recognize two observational selection effects which contribute to this bias. First, observers with limited observing time will prefer to follow rapidly changing objects, and thus may ignore those which are unresolved or show no changes in two epochs. This produces a deficit of slow sources. Second, one source (4C 39.25) which was a stable double for many years suddenly developed a moving component, and now is credited with a high proper motion. Thus, some of the other stable sources may have the potential for high proper-motion components, and are currently mislabeled. These selection effects are not quantifiable, but are in opposite directions. We believe that they contribute only a minor amount to the bias.

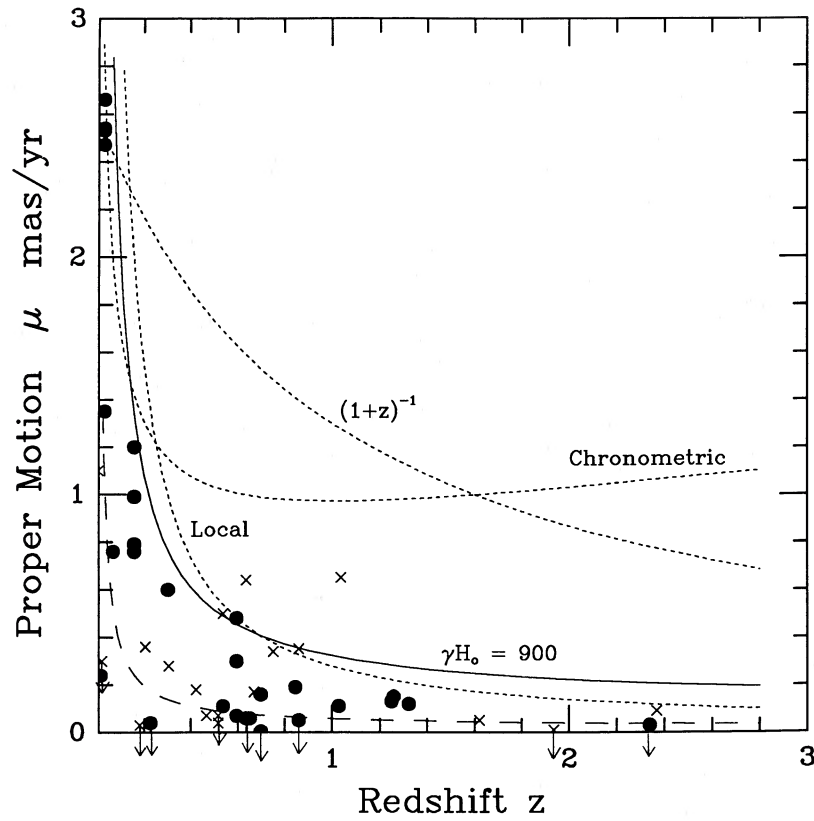


FIG. 1a

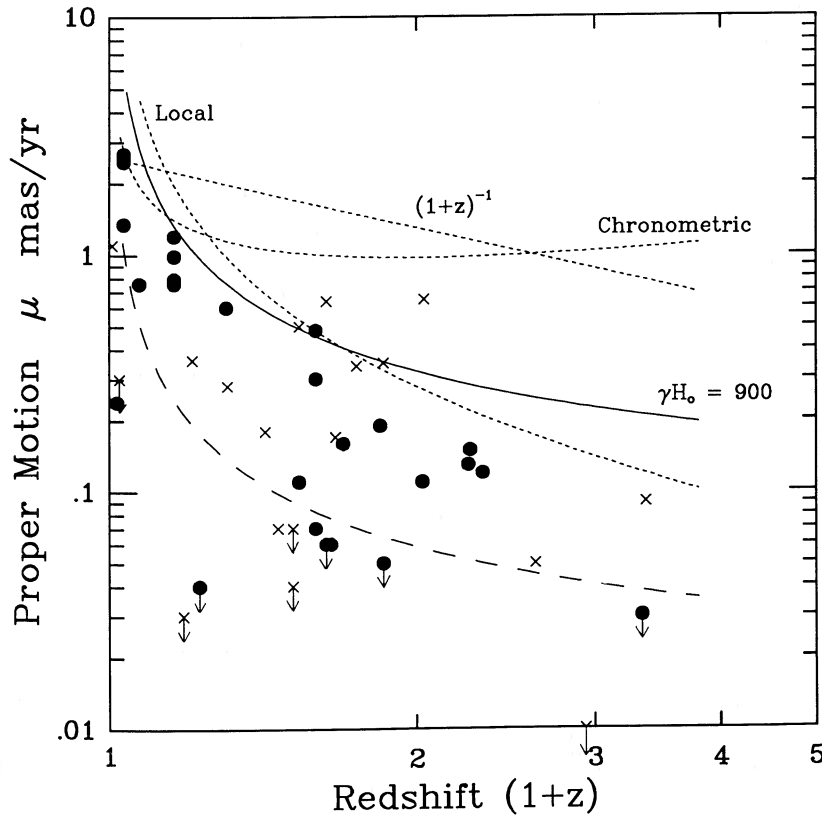


FIG. 1b

FIG. 1.—The μ - z diagram for 32 sources with measured internal proper motion. The solid line shows the limiting proper motion in a Friedmann universe for objects with one stationary component and another moving with Lorentz factor γ . The dashed line shows the proper motion for a component with $\gamma = 4$ moving at a fixed angle $\theta = 60^\circ$ to the line of sight, for $H_0 = 100 \text{ km s}^{-1} \text{ Mpc}^{-1}$ and $q_0 = 0.50$. The $(1+z)^{-1}$ line is the limiting proper motion in a local theory of quasars. The line marked "Local" refers to a Galaxy-centered model. The "Chronometric" line is the limiting proper motion in the chronometric theory, for $R/\beta_{\text{chron}} = 65 \text{ Mpc}$. (a) Linear scales; (b) logarithmic scales.

The two physical effects which have been discussed in the literature are Doppler boosting, which strengthens objects moving toward us and weakens those moving away; and toroidal shadowing, in which clear lines of sight are only obtained near the axis. The latter possibility seems unlikely, because the moving components are seen out to 100 pc (allowing for deprojection), and models of the narrow-line region do not allow significant absorption or scattering at these radii. Furthermore, we are in any event dealing with large values of γ , and thus we assume that Doppler boosting is mainly responsible for our bias for objects pointing at us. Doppler boosting is due to high-speed motion of the emitting fluid, but the proper motions we have been discussing are due to high-speed motions of a pattern. In general these are different (Lind and Blandford 1985) and in the extreme case they might be uncoupled. Our results, however, show that if the relativistic jet model is basically correct, then Doppler boosting plays an important role.

iv) *Relativistic Cosmology; Diverging Field*

There are possibilities other than the high-speed jet within the framework of relativistic cosmology. An ingenious class of models is those with a diverging or fountain-like field, where we see tangent points as they are successively excited by an expanding wave (Scheuer 1984). The dipole field was worked out in detail by Sanders (1974) and Bahcall and Milgrom (1980). The bound to the observed proper motion is still equation (2), but with $\gamma = 4.4$. However, equation (2) is now a *lower* bound, and the distribution should become sparse as μ increases. This does not fit Figure 1, unless $H_0 \leq 40 \text{ km s}^{-1} \text{ Mpc}^{-1}$. Furthermore, the well-established points below the limit imply either an unacceptably low value for H_0 or another mechanism which produces small values of proper motion.

A variant of this model has one fixed component, the central hot spot, and a moving component corresponding to the tangent wave from below the equatorial plane (Fig. 1 of Bahcall and Milgrom 1980). In this case the limit is an *upper* bound with $\gamma = 2.2$. This would require $H_0 \geq 300$ which is unacceptably high.

III. CONCLUSIONS

The available data demonstrate a strong anticorrelation between redshift and internal proper motion for compact radio sources. This is a direct indication that redshift is a measure of distance. This evidence is independent of the Hubble law, which utilizes a different correlation, that between redshift and apparent magnitude. Standard relativistic cosmology, in which redshift measures distance, supports the observed correlation between μ and z . A purely local theory in which quasars were all expelled from the galactic center at a common time in the past could also fit the data. However, there are various reasons

for believing that quasars are at great distances; probably the strongest is the chain of evidence which places galaxies far away, and the demonstration that many quasars are surrounded by a host galaxy.

Chronometric cosmology gives a limiting proper motion proportional to $(1+z)z^{-1/2}$. This predicts that proper motions will tend to increase with z for $z > 1$, which does not appear to match the observations. A model in which all quasars are at the same distance gives a limiting proper motion proportional to $(1+z)^{-1}$, which also does not match the data.

It has long been realized that cosmological tests that are independent of the Hubble law can be made if distant objects contain a standard measuring rod. Studies of "largest angular size" attempt to do this (e.g., Kapahi 1987). Here we have a related phenomenon, since proper motion is the derivative of the length of a measuring rod, and our "standard" is the constant Lorentz factor in the beaming model. In fact, however, since we discussed only limits to the proper motion, our standard can be the upper limit to the distribution of Lorentz factors. Our result that a chronometric cosmology does not match the proper motion data is consistent with Kapahi's similar result for median angular size. Kapahi also finds an increasing departure from Friedmann cosmology for $z \geq 1$; this is customarily ascribed to evolution of the linear size with z . There is not yet enough data for us to make similar detailed studies with the proper motion.

We have shown that the relativistic beaming model provides a reasonable fit to the data, and gives an upper bound on $\gamma H_0 \sim 900$; i.e., for H_0 between 50 and 100, the upper bound on γ lies between 18 and 9. The sources are not oriented at random but are systematically aimed at us, which suggests that Doppler boosting has an important role in their selection. A model consisting of a spherical shock wave in a dipole field will not work unless the Hubble constant takes on extreme values.

Orr and Browne (1982) developed a "unified scheme" for flat-spectrum and steep-spectrum quasars based on beaming of a central component, and found $\gamma \sim 5$. This can be reconciled with our value, $\gamma = 9-18$, without increasing H_0 , in two ways. First, there presumably is a distribution of γ ; our value is at the upper end and is expected to be bigger than that of Orr and Browne, which represents the average. Second, Orr and Browne have found a beaming Lorentz factor based on Doppler boosting, whereas ours is a kinematic Lorentz factor based on pattern motions. The higher pattern velocity would suggest that shock waves might be responsible for the moving components.

This work was supported by NSF grant AST 85-09822. Earlier versions have been published by Cohen (1987), and by Cohen *et al.* (1987a). We are grateful for discussions with R. D. Blandford, S. P. Reynolds, and I. E. Segal.

APPENDIX

An observer at O , at rest in the coordinate system (x, y, z) sees an object Q at distance r , moving along the x -axis with velocity $v = \beta c$ (see Fig. 2). The object Q is at rest in coordinate system (x', y', z') , where x' is parallel to x . The (x, y) plane contains v and r , and the angle between v and r is α . The object emits a blob B with velocity u' having spherical coordinates (η', ϕ') relative to x' and y' .

The observer sees a proper motion μ of B relative to Q , and interprets this as an apparent transverse velocity $\beta_{\perp} = \mu r/c$. A comoving observer (one at rest in the frame Q) sees a different proper motion μ' with transverse velocity $\beta_{\perp}' = \mu' r'/c$. The general formula for β_{\perp}' is (e.g., Pearson and Zensus 1987)

$$\beta_{\perp}' = \frac{\beta_b' \sin \theta'}{1 - \beta_b' \cos \theta'} \quad (\text{A1})$$

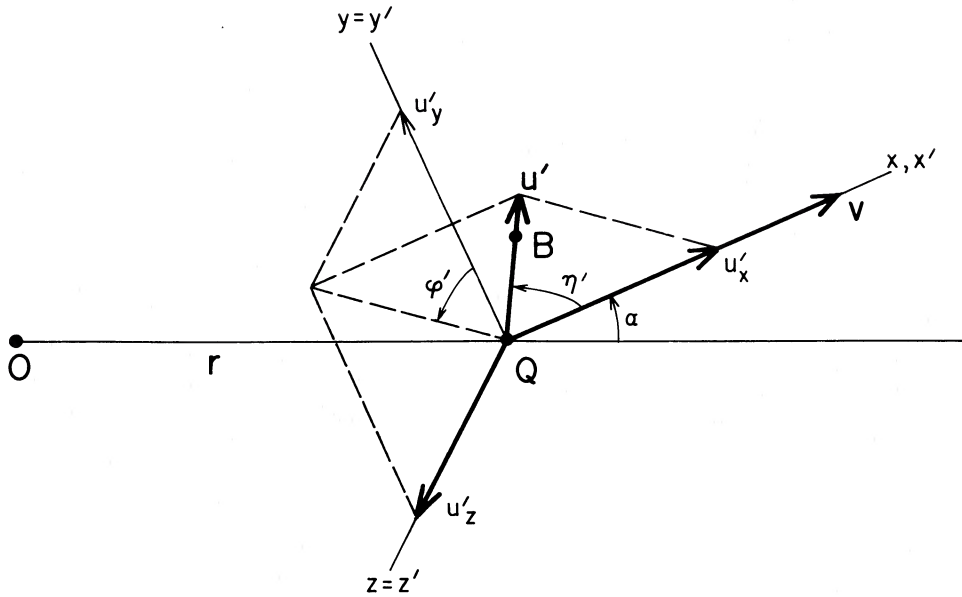


FIG. 2.—Coordinate systems

where $\beta'_b = u'/c$ and θ' is the angle between u' and the line to the comoving observer. For a fixed velocity u' , β'_\perp is maximized for $\cos \theta' = \beta'_b$, and in this case $\beta'_\perp = \beta'_b \gamma'_b = [(\gamma'_b)^2 - 1]^{1/2}$.

Consider first the special case $\alpha = 0$, with a fixed value for u' . Measurement time intervals in the two coordinate systems differ by the Doppler factor $(1+z) = (1+\beta)^{1/2}/(1-\beta)^{1/2}$ so that $\beta_\perp = \beta'_\perp/(1+z)$, and the maximum value for μ is

$$\mu_m = r^{-1} c \beta'_b \gamma'_b / (1+z). \quad (\text{A2})$$

For fixed distance and fixed ejection velocity the upper bound to the observed proper motion will vary as $1/(1+z)$.

Now consider the general problem of maximizing μ by varying η' when v and u' are fixed, but α , η' , and ϕ' are arbitrary. In the O -frame the blob has velocity u with components u_x , u_y , and u_z given by

$$\begin{aligned} u_x &= \frac{v + u' \cos \eta'}{1 + \beta \beta'_b \cos \eta'} \\ u_y &= \frac{u' \sin \eta' \cos \phi'}{\gamma(1 + \beta \beta'_b \cos \eta')} \\ u_z &= \frac{u' \sin \eta' \sin \phi'}{\gamma(1 + \beta \beta'_b \cos \eta')} \end{aligned} \quad (\text{A3})$$

where $\gamma = (1 + \beta^2)^{-1/2}$. In frame O the angle θ between u and the line of sight (from Q to O) is given by

$$u \cos \theta = u_y \sin \alpha - u_x \cos \alpha, \quad (\text{A4})$$

and $\mu = \beta_\perp c/r$, where

$$\beta_\perp = \frac{(u/c) \sin \theta}{1 - (u/c) \cos \theta}. \quad (\text{A5})$$

We found the maximum of μ numerically, by picking α and ϕ' and calculating β_\perp as a function of η' . When ϕ' is small enough there are two local maxima for $\beta_\perp(\eta')$, corresponding to emission of B above and below the (r, z) plane. The average of these local maxima is just μ_m (eq. [A2]). When ϕ' is large enough there is only one maximum, which is smaller than μ_m . In general, μ has a maximum for $\phi' = 0$; the maximum increases with α and for α large enough, can actually increase with z . In Figure 1 we have plotted $\mu_m \propto (1+z)^{-1}$ which represents the fastest possible decrease of μ with z .

Equation (A2), the case where Q moves directly away from the observer, can be derived by setting $\alpha = \phi' = 0$, and substituting equations (A3) and (A4) into (A5).

REFERENCES

- Bääth, L. B. 1984, in *IAU Symposium 110, VLBI and Compact Radio Sources*, ed. R. Fanti, K. Kellermann, and G. Setti (Dordrecht: Reidel), p. 127.
 ———, 1987, in *Superluminal Radio Sources*, ed. J. A. Zensus and T. J. Pearson (Cambridge: Cambridge University Press), p. 206.
 Bahcall, J. N., and Milgrom, M. 1980, *Ap. J.*, **236**, 24.
 Barthel, P. D. 1987, in *Superluminal Radio Sources*, ed. J. A. Zensus and T. J. Pearson (Cambridge: Cambridge University Press), p. 148.
 Barthel, P. D., Pearson, T. J., Readhead, A. C. S., and Canzian, B. J. 1986, *Ap. J. (Letters)*, **310**, L7.
 Biretta, J. A., Moore, R. L., and Cohen, M. H. 1986, *Ap. J.*, **308**, 93.

- Biretta, J. A., and Reid, M. J. 1988, in Proc. Conference on Active Galactic Nuclei, Georgia State University, Atlanta, in press.
- Cohen, M. H. 1987, in *Superluminal Radio Sources*, ed. J. A. Zensus and T. J. Pearson (Cambridge: Cambridge University Press), p. 306.
- Cohen, M. H., Barthel, P. D., Pearson, T. J., and Zensus, J. A. 1987a, in *IAU Symposium 129, The Impact of VLBI on Astrophysics and Geophysics*, ed. M. Reid and J. Moran (Dordrecht: Reidel), in press.
- Cohen, M. H., Zensus, J. A., Biretta, J. A., Comoretto, G., Kaufmann, P., and Abraham, Z. 1987b, *Ap. J. (Letters)*, **315**, L89.
- Cotton, W. D., Counselman, C. C., III, Geller, R. B., Shapiro, I. I., Wittels, J. J., Hinteregger, H. F., Knight, C. A., Rogers, A. E. E., Whitney, A. R., and Clark, T. A. 1979, *Ap. J. (Letters)*, **229**, L115.
- Eckart, A., Witzel, A., Biermann, P., Pearson, T. J., Readhead, A. C. S., and Johnston, K. J. 1985, *Ap. J. (Letters)*, **296**, L23.
- Hough, D. H., and Readhead, A. C. S. 1987, *Ap. J. (Letters)*, **321**, L11.
- Jones, D. L. 1986, *Ap. J. (Letters)*, **309**, L5.
- Kapahi, V. 1987, in *IAU Symposium 124, Observational Cosmology*, ed. A. Hewitt, G. Burbidge, and L. Z. Fang (Dordrecht: Reidel), p. 251.
- Lind, K. R., and Blandford, R. D. 1985, *Ap. J.*, **295**, 358.
- Marscher, A. P., and Broderick, J. J. 1985, *Ap. J.*, **290**, 735.
- Mutel, R. L., and Phillips, R. B. 1987, in *Superluminal Radio Sources*, ed. J. A. Zensus and T. J. Pearson (Cambridge: Cambridge University Press), p. 60.
- Orr, M. J. L., and Browne, I. W. A. 1982, *M.N.R.A.S.*, **200**, 1067.
- Pauliny-Toth, I. I. K., Porcas, R. W., Zensus, J. A., and Kellermann, K. I. 1984, in *IAU Symposium 110, VLBI and Compact Radio Sources*, ed. R. Fanti, K. Kellermann, and G. Setti (Dordrecht: Reidel), p. 149.
- Pauliny-Toth, I. I. K., Porcas, R. W., Zensus, J. A., Kellermann, K. I., Wu, S. Y., Nicolson, G. D., and Mantovani, F. 1987, *Nature*, **328**, 778.
- Pearson, T. J., Barthel, P. D., Lawrence, C. R., and Readhead, A. C. S. 1986, *Ap. J. (Letters)*, **300**, L25.
- Pearson, T. J., Readhead, A. C. S., and Barthel, P. D. 1987, in *Superluminal Radio Sources*, ed. J. A. Zensus and T. J. Pearson (Cambridge: Cambridge University Press), p. 94.
- Pearson, T. J., and Zensus, J. A. 1987, in *Superluminal Radio Sources*, ed. J. A. Zensus and T. J. Pearson (Cambridge: Cambridge University Press), p. 1.
- Porcas, R. W. 1987, in *Superluminal Radio Sources*, ed. J. A. Zensus and T. J. Pearson (Cambridge: Cambridge University Press), p. 12.
- Preuss, E., and Alef, W. 1987, in *IAU Symposium 129, The Impact of VLBI on Astrophysics and Geophysics*, ed. M. Reid and J. Moran (Dordrecht: Reidel), in press.
- Readhead, A. C. S., Pearson, T. J., and Unwin, S. C. 1984, in *IAU Symposium 110, VLBI and Compact Radio Sources*, ed. R. Fanti, K. Kellermann, and G. Setti (Dordrecht: Reidel), p. 131.
- Roberts, D. H., and Wardle, J. F. C. 1987, in *Superluminal Radio Sources*, ed. J. A. Zensus and T. J. Pearson (Cambridge: Cambridge University Press), p. 193.
- Romney, J. D., Alef, W., Pauliny-Toth, I. I. K., Preuss, E., and Kellermann, K. I. 1984, in *IAU Symposium 110, VLBI and Compact Radio Sources*, ed. R. Fanti, K. Kellermann, and G. Setti (Dordrecht: Reidel), p. 137.
- Sanders, R. H. 1974, *Nature*, **248**, 390.
- Scheuer, P. A. G. 1984, in *IAU Symposium 110, VLBI and Compact Radio Sources*, ed. R. Fanti, K. Kellermann, and G. Setti (Dordrecht: Reidel), p. 197.
- Segal, I. E. 1979, *Ap. J.*, **227**, 15.
- Shaffer, D. B., and Marscher, A. P. 1987, in *Superluminal Radio Sources*, ed. J. A. Zensus and T. J. Pearson (Cambridge: Cambridge University Press), p. 67.
- Simon, R. S., Johnston, K. J., Hall, J., Spencer, J. H., and Waak, J. A. 1987, in *Superluminal Radio Sources*, ed. J. A. Zensus and T. J. Pearson (Cambridge: Cambridge University Press), p. 72.
- Terrell, J. 1975, in *Theories and Experiments in High-Energy Physics*, ed. B. Kursunoglu, A. Perlmutter, and S. M. Widmayer (New York: Plenum), p. 457.
- Unwin, S. C. 1987, in *Superluminal Radio Sources*, ed. J. A. Zensus and T. J. Pearson (Cambridge: Cambridge University Press), p. 34.
- Unwin, S. C., Cohen, M. H., Biretta, J. A., Pearson, T. J., Seielstad, G. A., Walker, R. C., Simon, R. S., and Linfield, R. P. 1985, *Ap. J.*, **289**, 109.
- Walker, R. C. 1986, *Canadian J. Phys.*, **64**, 452.
- Witzel, A. 1987, in *Superluminal Radio Sources*, ed. J. A. Zensus and T. J. Pearson (Cambridge: Cambridge University Press), p. 83.
- Zensus, J. A., Hough, D. H., and Porcas, R. W. 1987, *Nature*, **325**, 36.
- Zensus, J. A., and Pearson, T. J. 1987, in *IAU Symposium 129, The Impact of VLBI on Astrophysics and Geophysics*, ed. M. Reid and J. Moran (Dordrecht: Reidel), in press.
- Zensus, J. A., and Porcas, R. W. 1987, in *Superluminal Radio Sources*, ed. J. A. Zensus and T. J. Pearson (Cambridge: Cambridge University Press), p. 126.

P. D. BARTHEL, M. H. COHEN, T. J. PEARSON, and J. A. ZENSUS: California Institute of Technology, Mail Code 105-24, Pasadena CA 91125